J. Phys. B: At. Mol. Phys. 17 (1984) 3295–3310. Printed in Great Britain

A measurement of the cross section for ionisation of helium by electron impact using a fast crossed beam technique

R G Montague, M F A Harrison and A C H Smith†

Culham Laboratory (Euratom/UKAEA Fusion Association), Abingdon, Oxon, OX14 3DB, UK

Received 20 January 1984

Abstract. The cross section for the single ionisation of ground state helium atoms by electron impact has been measured over the energy range from threshold to 750 eV using a crossed electron–fast atom beam technique. The absolute value of the measured cross section is estimated to be accurate to within about ±6% at a 90% confidence level. Ionisation contributions from excited atoms are negligible. These data are in excellent agreement with those of Rapp and Englander-Golden who applied the electron beam–static-gas target technique. The mean of these two cross sections is recommended as the best data currently available for ionisation of helium. The experimental procedure is fully described and a detailed assessment is made of the experimental errors.

1. Introduction

The primary objective of the present study has been to obtain a precise absolute measurement of the electron impact ionisation cross section of atomic helium using the crossed electron–fast atom beam technique and to compare the data with published results of beam–static-gas experiments. The basic fast atom beam approach was first used by Cook and Peterson (1962) to study atomic nitrogen but it has more recently been improved and more widely applied in the present authors' laboratory for electron impact ionisation of metastable atoms (Dixon *et al* 1975, 1976) and ground state atoms (Brook *et al* 1978). The latter study included some measurements on helium primarily to verify the method before proceeding with the main study of ionisation of atoms of carbon, nitrogen and oxygen. Since that time some very significant improvements have been made in the equipment and operating procedures. A secondary objective of the present study has therefore been to identify the limitations to the absolute accuracy of cross section measurements now attainable with this technique.

Ionisation of helium by electron impact is a common process in natural plasmas. In man-made plasmas it is particularly relevant to controlled thermonuclear fusion devices because helium is the atomic product of the D–T fusion reaction. It is also the simplest terrestrial atomic gas and the helium atom is therefore a natural candidate for use as a standard for measured atomic collision data. Moreover, this atom provides a good testing ground for atomic collision theory because accurate multi-parameter wavefunctions are now available and the ionisation is not complicated by inner shell effects, although autoionisation through excitation of both electrons makes a small contribution to the total ionisation.

† Department of Physics and Astronomy, University College London, London WC1E 6BT, UK.

0022-3700/84/163295+16$02.25

Many previous absolute measurements of the ionisation cross section of helium by electron impact have been made†. Those published up to 1965 have been critically reviewed by Kieffer and Dunn (1966). Prior to 1978 all absolute measurements of the ionisation cross section were made using the beam–static-target technique in which an electron beam is passed through a cell containing helium gas. The total ionisation cross section is determined from measurements of the generated ion current, the incident electron current, the gas pressure and the length of the electron beam over which the ions are produced. This total ionisation cross section is defined by $Q_T(e) = \Sigma_n nQ_n(E)$, where $Q_n(E)$ is the cross section for producing an ion of the nth degree of ionisation at an incident electron energy E. The method, originated by Jones (1927), was developed by Tate and his coworkers (e.g., Tate and Smith 1932) and it has been widely used for measurements of ionisation cross sections of many atoms and molecules. There are major discrepancies between the published data but the experiments of Rapp and his coworkers (e.g., Rapp and Englander-Golden 1965) represent a particularly careful application of this method and for helium a maximum possible error of 7% is quoted. Verification of the absolute accuracy of Rapp and Englander-Golden's data for helium atoms would therefore provide powerful indirect support for a wide base of published ionisation data.

The beam–static-target technique can be subject to a number of errors. In particular the length of the electron trajectories within the ion collection region is uncertain due to the presence of the magnetic field which is used to collimate the beam. Electron scattering and the suppression of secondary electrons may also cause problems and there may be errors in the estimated target density due to difficulties in measuring gas pressures in the range 10^{-4} to 10^{-2} Torr. The crossed electron–fast atom beam technique is free from these sources of error because magnetic fields are not needed to guide the electrons, the number density of the target atoms is determined from their flux and velocity, and the collision volume and beam density profiles are precisely known. Magnetic selection of the product ion ensures that only the single-process cross section $Q_I(E)$ is measured and not the total ionisation cross section $Q_T(E)$. However, there are difficulties in producing a target beam which contains only ground state atoms. The target beam is produced by charge exchange of the parent ion beam in a gas cell and the neutral component may contain both metastable and long-lifetime highly-excited atoms. This excited atom population can be substantially reduced by a combination of electric field ionisation, careful alignment of the target beam through the charge exchange cell, and operation at relatively low ion beam energy (typically 2 keV). Some control over the presence of metastable atoms can also be exercised by choice of the charge exchange gas.

The preliminary crossed electron–fast atom beam measurements by Brook *et al* of the ionisation cross section of helium are in reasonably good agreement with those of Rapp and Englander-Golden at energies above 50 eV after making allowance for the contribution of double ionisation. However, between this energy and the threshold, the cross section was found to be significantly and progressively smaller. Brook *et al* suggested that the discrepancy might be due to the effects introduced by magnetic collimation of the electron beam in Rapp and Englander-Golden's experiment but, on the other hand, Harrison *et al* (1979) emphasised the need for eliminating ambiguities due to poor counting statistics and contributions from excited helium atoms in the

† We exclude from the discussion indirect determinations from measurements of Townsend ionisation coefficients.

near-threshold region. It will be seen that these problems no longer exist as a result of the improved apparatus and procedures used in the present experiment.

2. Apparatus, method and experimental procedure

2.1. The crossed beams method

A schematic diagram of the beam system is presented in figure 1. A beam of He^+ ions is extracted at 2 or 4 keV from a PIG source†, focused with an einzel lens, and mass-selected with a 60°-sector magnetic field. It then traverses a tightly collimating

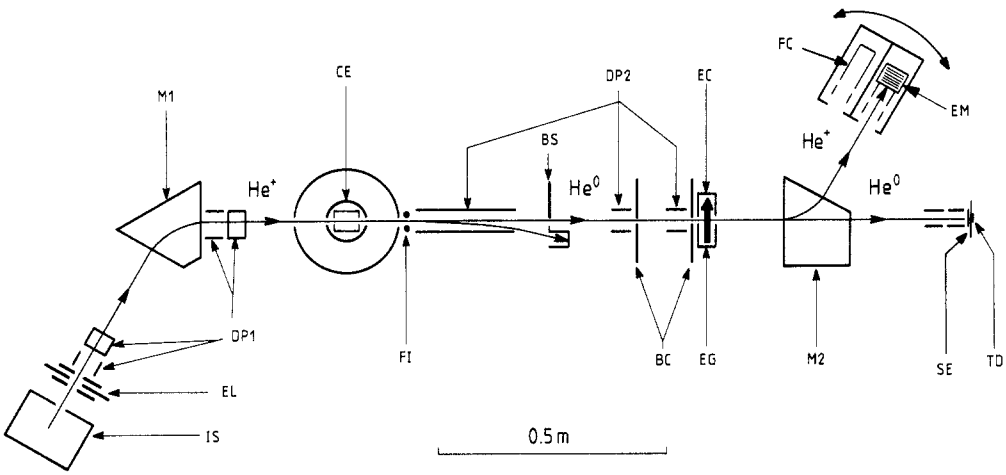

Figure 1. Schematic diagram of the crossed beams apparatus: IS ion source (electron bombardment PIG type), EL einzel lens, DP1 deflector plates to optimise path of ion beam, M1 ion selector magnet, CE charge exchange cell containing helium gas, FI field ioniser bars to ionise highly excited atoms, DP2 electrostatic deflector plates to remove ions from atom beam, BS beam stop aperture, BC beam collimators, EG electron gun, EC electron collector, M2 analyser magnet, SE secondary electron emission detector for fast helium atoms (aluminium target surface), TD integral thermopile used for calibration of SE, EM electron multiplier for detection of He^+ product ions, FC Faraday cup for calibration of the electron multiplier.

charge exchange cell containing helium gas, in which about 10% of the ions are converted to helium atoms. The remaining ions are electrostatically deflected out of the atom beam which then enters the collision region where it is intersected at 90° by an electron beam. After leaving the collision region, the atom beam enters a calibrated detector (described in more detail in the appendix) and the electron beam is collected in a Faraday cup. He^+ product ions are separated from the atom beam with a second 60°-sector magnet and are detected with a calibrated electron multiplier. Charge pulses from the electron multiplier are processed and counted using a conventional arrangement of amplifier, discriminator and scalers. Further details of the apparatus and method are given in earlier papers (Dixon *et al* 1975, 1976, Brook *et al* 1978).

† A hot cathode arc with an axial magnetic field.

The present apparatus and the experimental method are basically those used by Brook *et al* (1978), but the operational procedures have been modified to take advantage of an on-line computer system (CTL Modular One with CAMAC interface). This is used for storing and processing data and for controlling the electron gun, the beam pulsing and the particle detection electronics. Other changes include the installation of an ion beam position feedback system to improve the stability of the target beam, improved alignment of the apparatus by means of a laser, and improved vacuum conditions.

A significant problem in these experiments was initially the presence of long-lived highly-excited atoms in the parent helium atom beam. It was found that the concentration of excited atoms could be reduced by careful collimation of the beam through and after the charge exchange cell. This implies that electron capture into excited states is accompanied by scattering. The charge exchange cell used in these experiments is a tube 57 mm in length with sharp-edged apertures 2.8 mm high and 2.0 mm wide at both entry and exit. The cell is supplied with helium at its centre and the effusing gas is inhibited from entering the main vacuum system by two differential pumping stages arranged concentrically around the cell.

In this experiment background counts from extraneous collisions were detected by the He^+ ion detector when the atom beam was present, but the electron beam did not produce extraneous counts. Thus to separate the signal due to beam collisions from the background it was necessary to modulate the electron beam. In these circumstances the expression for the cross section in terms of the experimental parameters is

$$Q(E) = \frac{e^2 h' S \gamma_0}{\bar{I}\bar{J}t\Omega} \frac{vV}{(v^2+V^2)^{1/2}} \tag{1}$$

where

S is the number of He^+ signal counts (corrected for dead time) accumulated by the counting system during an experimental period t;
$\bar{I}$ is the time-averaged output current from the neutral beam detector;
$\bar{J}$ is the time-averaged electron current including the defining slit plate current $\bar{J}_{ds}$ (see § 2.2);
Ω is the efficiency of the product ion detector;
γ_0 is the neutral detector efficiency;
v and V are the velocities of electrons and atoms respectively;
E is the incident electron kinetic energy $[\frac{1}{2}m(v^2+V^2)]$;
m is the mass of the electron;
e is the electronic charge;
h' is the effective height of the atom beam in the collision region and is given by

$$h' = \left(\int_{-\infty}^{\infty} i(z)\,dz \int_{-\infty}^{\infty} j(z)\,dz\right)\left(\int_{-\infty}^{\infty} i(z)j(z)\,dz\right)^{-1}$$

where z is the coordinate perpendicular to the axes of the two beams and $i(z)$ and $j(z)$ are the currents per unit height of the atom and electron beams respectively.

2.2. Measurement of the experimental parameters

The methods of measurement of the parameters of equation (1) are described below and typical magnitudes and errors are given in tables 1 and 2.

S and t. Charge pulses from the electron multiplier (Johnston Laboratories, type MM1) are amplified and then fed to a discriminator which has a well defined dead time (usually set to 1 μs and discussed further in connection with Ω) and then to the common input of a pair of scalers. The scalers are alternately gated (pulse length 488 μs, 50% duty cycle) in order to separate the signal from background. The electron beam pulses are made slightly shorter (10 μs) than the open-gate periods of the scalers. In this single-beam pulsing mode it is unnecessary to know the exact duration of the electron beam pulses; only the time-averaged current $\bar{J}$ needs to be measured. S is the difference between the scaler readings in a counting period t after correcting for the dead time of the counting system. Both t and the gating period are derived from a crystal-controlled pulse generator (frequency 2^{24} Hz) and timing errors are negligible. The signal counts are directed alternately to each scaler in successive counting periods so that any possible error from inequalities in the response of the scalers is cancelled.

$\bar{I}$. The current from the atom beam detector is fed to a vibrating capacitor electrometer (Carey Instruments, model 401) whose output is connected to a voltage-to-frequency converter (VFC) coupled to a scaler. The scaler is activated for the experimental time period t so that the recorded counts are proportional to the current averaged over the period t. The system is calibrated by recording the output counts when a known input current is applied from a calibrated current source (Keithley, model 261).

$\bar{J}$. The electron beam current is determined from the potential developed across a precision resistor (±0.1%). This voltage is fed to a second gated VFC/scaler combination, so that the total counts recorded are again proportional to the time-averaged current. The system is calibrated with a calibrated voltage source (Time Electronics, model 2003). A defining slit plate is positioned in front of the electron collector

Table 1. Typical values of parameters in equation (1).

Parameter	Value	Electron energy	Atom energy	Note
S	$10\ s^{-1}$	29 eV	2 keV	(a)
	$200\ s^{-1}$	118 eV	2 keV	(a)
	$100\ s^{-1}$	550 eV	2 keV	(a)
t	2048 s			(b)
Ω	0.79 ± 0.03		2 keV	
	0.87 ± 0.02		4 keV	
γ_0	0.80 ± 0.03		2 keV	
	1.12 ± 0.02		4 keV	
h'	2.50 ± 0.05 mm			
$\bar{I}$	4.5 nA		2 keV	(c)
	8.0 nA		4 keV	(c)
$\bar{J}$	93 μA	29 eV		(a)
	248 μA	118 eV		(a)
	206 μA	550 eV		(a)

(a) Maximum value.
(b) Value of t for most of the experimental points in figure 4.
(c) Typical value.

Table 2. Errors in the values of parameters in equation (1).

(1) Systematic errors compounded from errors inherent in the method and from instrument calibration errors.

Parameter	Error (%) expressed as calculated or estimated 90% confidence limits
S	negligible
t	negligible
Ω	±2.0
γ_0	±3.8
h'	±1.5
V	±0.3
$\bar{I}$	±0.5
$\bar{J}$	±1.0
Total	±4.7

(2) Random errors arising from variability of γ_0 and Ω and the statistical error of the recorded ion count rate.

Electron energy range	<30 eV	30–40 eV	40–100 eV	100–150 eV	150–400 eV	400–750 eV
Error (90% confidence limits)	$\pm 4 \times 10^{-19}$ cm^2	±4%	±3%	±1%	±3%	±4.5%

(3) Total error compounded from systematic and random errors. This represents the error on the best curve drawn through the experimental points (see figures 3 and 4 and table 3).

Electron energy range	<30 eV	30–40 eV	40–100 eV	100–150 eV	150–400 eV	400–750 eV
Error (90% confidence limits)	$\pm 4 \times 10^{-19}$ cm^2	±6.2%	±5.6%	±4.8	±5.6%	±6.5%

described by Dixon *et al* (1976); the slit is smaller in height than the atom beam so that if all of the electron beam passes through the atom beam then the current J_{ds} to the slit plate should be zero. In practice this ideal condition cannot be achieved, but J_{ds} does not exceed a few per cent of the total J for the data reported here. It is probable (and there is experimental evidence to support this) that most of the electrons that strike the slit plate have passed through the atom beam, so J_{ds} has been added to the collector current to obtain the total beam current, J. The plate is normally at earth potential, so any secondary electrons emitted from it will affect the measurements of J_{ds}. To avoid this problem, $\bar{J}_{ds}$ (the time-averaged current) is measured before each experimental run by biassing the plate typically to +4 V thereby suppressing the secondary emission. The existence of $\bar{J}_{ds}$ introduces an uncertainty into $\bar{J}$ which is represented in our judgement by ±0.5 $\bar{J}_{ds}$ (90% confidence limits).

Ω. To measure the He^+ detection efficiency (counts/ion), the electron multiplier detector is moved out of the path of the He^+ ions and is replaced by a deep Faraday cup (see Dance *et al* (1967) for details of system). The cup is connected to the electrometer/VFC combination normally used for measuring $\bar{I}$. A weak beam of He^+ ions ($\sim 10^{-14}$ A) is passed through the apparatus and is alternately collected by the

electron multiplier or by the Faraday cup usually for several periods each of 16 s. The procedure is repeated for several values of ion current. The values of Ω and the dead time τ are deduced from the intercept and gradient of a graph C/P against C, where C is the count rate recorded by the scaler connected to the electron multiplier and P is the equivalent count rate deduced by dividing the current collected by the Faraday cup by e (the electronic charge). A typical set of results is shown in figure 2.

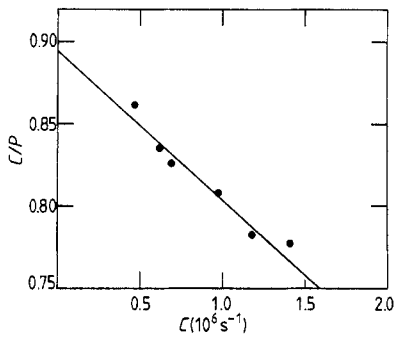

Figure 2. Typical set of data used for calibration of the electron multiplier detector. See text for explanation. $\Omega = 0.894 \pm 0.017$, $\tau = 1.02 \pm 0.02$ μs.

The value of Ω thus determined is only accepted if the value of τ agrees (within 90% confidence limits) with the known value set at the discriminator. Departures from the correct value of τ signify instabilities in the ion current during the calibration procedure. The value of Ω was determined with 90% confidence limits of $\pm 2\%$ and the calibration was repeated many times during the course of obtaining the ionisation data presented here. A slow drift in the value of Ω was observed and the best value at the time of a particular ionisation measurement was therefore determined by interpolation between the measured values. This interpolation does not significantly increase the 90% confidence limits which in our judgement remain as $\pm 2\%$.

γ_0. The efficiency of the neutral beam detector (which in effect is the value of the secondary emission coefficient of the aluminium surface averaged over the area impacted by the helium atom beam) was measured at intervals of a few hours during the course of the experiment. The procedure together with a description of the detector is given in the appendix. γ_0 was found to be the least stable parameter in equation (1) and the uncertainty in its value is the main contribution to the overall uncertainty in the measured cross section. The cause of the drift and instability of γ_0 was the subject of a prolonged investigation. It seems that initially the secondary electron emission of a new detector changed with time when the surface was bombarded with the helium beam, but eventually a central region with an adequately stable but inhomogeneous secondary emission coefficient was formed. If the atom beam was slightly re-aligned or the parent ion beam was differently focused, a different value of the average γ_0 would then be observed. In order to determine the most appropriate value of γ_0 for each particular ionisation measurement, the measured γ_0 values were plotted as a function of time and a smooth curve was drawn through the points. The value of γ_0 at the appropriate time was then taken from the curve. Ninety per cent confidence limits on γ_0 were estimated from the scatter of the points. Even so, as will be seen in § 3, different sets of ionisation data did not quite match each other in

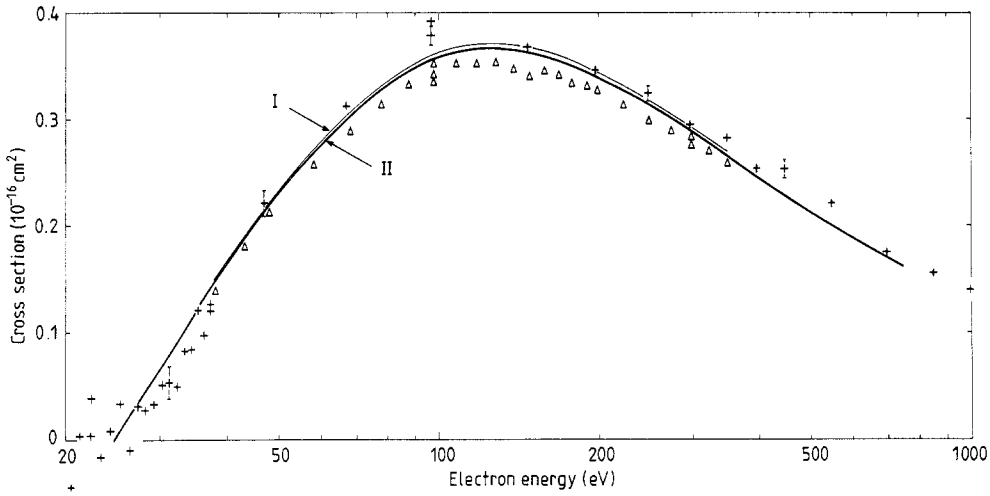

Figure 3. Curve I is a smooth curve drawn through the normalised points (not shown) of data sets (b) and (c). The triangles (Δ) are the points of set (a); the statistical errors (90% confidence limits) are approximately equal to the vertical dimension of the triangles. Curve II is a smooth curve drawn through the finally normalised points of data sets (a), (b) and (c) and represents the best absolute cross section obtainable from the present data (see also figure 4). The crosses (+) are the data points of Brook *et al* (1978); the error bars shown for these particular data at selected points are typical statistical errors (90% confidence limits).

absolute magnitude and weighted adjustments had to be applied. These discrepancies are probably attributable to the inability to determine the relevant value of γ_0 correctly (see § 5 also). Another source of error in determining γ_0 could be the reflection of energetic helium atoms or ions from the target surface. However, the reflection coefficients of atoms and ions at the energies employed are small and approximately equal (Eckstein and Verbeek 1979), so that the effects are compensating and no significant error in the measurement of γ_0 is likely to be introduced.

E and v. The incident electron collision energy (in electron volts) can be conveniently expressed as $E = -V_k + \delta + \varepsilon$ where V_k is the cathode potential of the electron gun relative to the collision region and ε is the contribution of the atom beam velocity (i.e. $\varepsilon = 1.36 \times 10^{-4} E_0$ where E_0 is the helium atom energy in electron volts). The potential δ arises from a combination of contact potentials, electric field penetration into the collision region and the initial velocities of the emitted electrons. Some recent measurements in the authors' laboratory, in which an energy analyser was used, show that a small variation of δ with V_k and J does occur, but the amount is negligible in the context of the present experiment. δ is therefore taken to be constant. Its mean value $\bar{\delta}$ is obtained by measuring the normalised ionisation signal $S/(\bar{I}\bar{J})$ as a function of V_k in the region of the ionisation threshold for helium and extrapolating the linearly decreasing signal back to the V_k axis.

The inset in figure 4 shows the data used to determine δ, which was found to be -2.3 ± 0.5 V. This value is consistent with values previously obtained with the same type of cathode (Harrison *et al* 1979). From the shape of the curve at the onset of ionisation it is seen that the electron energy spread is about 1 eV (FWHM) and is consistent with that estimated in earlier work (Dance *et al* 1966).

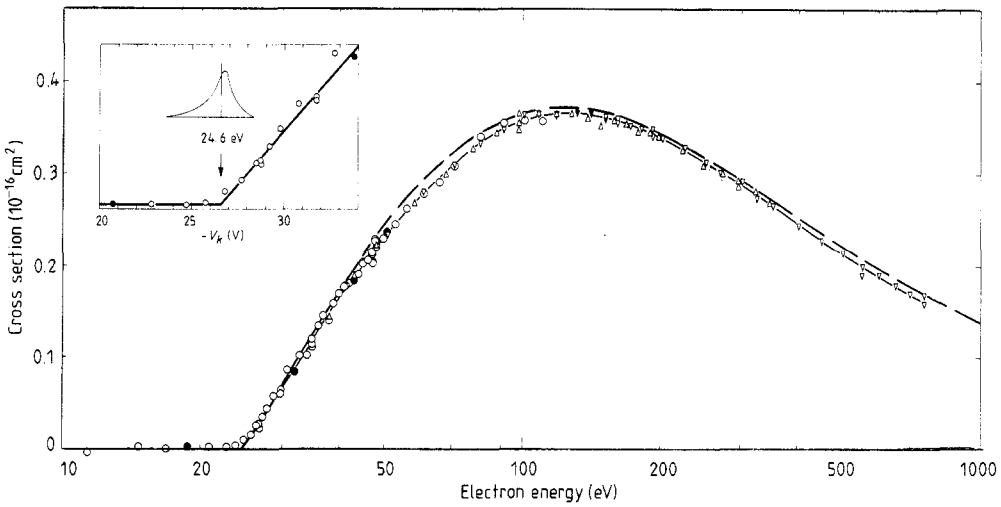

Figure 4. The cross section for ionisation of helium atoms by electron impact plotted against electron energy. Experimental points are the present results, △ for set (a); ○ for set (b); ▽ for set (c). Curves: —— best line through experimental points of present work; — — Rapp and Englander-Golden (1965) (experiment). Inset: near-threshold ionisation signal ($S/\bar{I}\bar{J}$) plotted against cathode potential (V_k) of the electron gun; these data were used to calibrate the electron energy (see § 2.2). The energy distribution of the electrons estimated by Dance *et al* (1966) for a similar cathode and electron gun system is also shown. The solid points represent between four and seven superimposed points.

The electron velocity v has only a small effect on the determination of $Q(E)$.

V. The helium atom velocity V is determined from the accelerating potential applied to the ion source. The high potential applied to the source anode is measured accurately (±0.1%) by means of a precision resistive divider and a digital voltmeter, but a small additional uncertainty arises from the uncertainty of the plasma potential in the ion source relative to the source anode. The overall error in V is not more than ±0.3%. Any change in the velocity of the helium particle in capturing an electron in the charge exchange neutralisation process is negligible.

h'. In order to determine the effective height of the atom beam, the intensities of both the atom and the electron beam are sampled simultaneously at each of 29 vertical positions by means of a shutter with a 0.15 mm slit. The shutter is driven through the beams by a micrometer drive coupled to a stepping motor. The computer controls the shutter scan and calculates the value of h'. The rapidity and ease with which a value of h' is now obtainable means that the beam profiles can be monitored frequently and the profile of the neutral beam can readily be made nearly uniform by means of the ion beam deflectors. In this condition, a change in the electron beam profile, which is far from uniform, does not introduce a significant change in the value of h'. The estimated 90% confidence limits of the values of h' thus obtained are ±1.5%.

The effective height h' is defined in terms of the atom beam intensity profile $i(z)$, but in practice it is measured in terms of a detected profile $i_d(z)$ of secondary electrons, where $i_d(z) = \gamma(z)\ i(z)$ and $\gamma(z)$ is the vertical distribution of the secondary emission coefficient at the neutral detector surface. If $\gamma(z)$ is not constant then an error occurs in the determination of h'. In order to assess the magnitude of such an error, the

secondary emission coefficient profile of He^+ ions, $\gamma^+(z)$, was measured by scanning a narrow 4 keV He^+ beam across the surface. It was found that $\gamma^+(z)$ was not constant, but if the profile $\gamma(z)$ of the corresponding atom beam coefficient is the same as $\gamma^+(z)$, then it is estimated that the error in the determination of h' will not exceed 2% and will generally be much less than this. Thus any inhomogeneity of $\gamma(z)$ is unlikely to introduce a significant additional error in the present data and so it is ignored in the overall error assessment presented in § 3.

2.3. Procedure for determining the cross section

The ionisation data for determining the cross section were obtained in two ways. Firstly, at each electron energy studied in the range above 50 eV, signals were usually measured at several electron currents $\bar{J}$. The normalised signal $S/\bar{I}$ was plotted on a graph against $\bar{J}$ in order to check the linearity. In all cases $S/\bar{I}$ was found to be linear with $\bar{J}$ within the statistical errors up to the maximum electron currents used. The intercepts of straight lines (of form $y = a + bx$) fitted to the points by the method of least squares were found to be not significantly different from zero (i.e. $a = 0$). The cross section values for all data obtained in this manner were therefore calculated from the gradients of straight lines through the origin (of form $y = bx$) by application of equation (1)†.

Secondly, at electron energies less than 50 eV and in some instances above 50 eV, the ionisation signal was measured at a single value of electron current for each electron energy and the cross section was determined by direct application of equation (1).

3. Results

Three sets of measurements were made:

(a) Initial observations using a 4 keV atom beam provided absolute measurements of the cross section at 28 values of collision energy ranging from 38 to 348 eV.

(b) Observations using a 2 keV atom beam were made in order to minimise any component of highly excited atoms. At the time it was also considered that long term drifts in calibration may have affected set (a) so, in order to provide greater confidence in the shape of the cross section, each data point of set (b) was compared with an accompanying absolute measurement at 118 eV and the data thereby made relative to that at 118 eV. The data of set (b) were taken over the range from 12.7 eV (i.e. well below threshold) up to 118 eV.

(c) The procedure adopted for set (b) was repeated using a 4 keV atom beam and collision energies ranging from 50.8 eV to 750 eV.

In sets (b) and (c) a total of 75 measurements of the cross section at 118 eV were obtained and the distribution of values is approximately normal with a standard deviation of 5%. The predominant cause of this distribution is the variability of γ_0 and to a lesser extent of Ω; it is not due to the statistical error of the signal counting measurements (at all energies greater than 33 eV the counting errors are much smaller than 5%). Because of the large number of absolute measurements made, it is possible to assign 90% confidence limits (which are based on the standard error of the mean)

† The justification is that if $S \neq 0$ for $J = 0$, then the data would not be acceptable. It is physcially unrealistic to allow S at $J = 0$ to be variable as would be the case if the data were fitted to a straight line of the form $y = a + bx$.

of only ±1% on the mean cross section value at 118 eV. Systematic errors, which are discussed elsewhere, must of course be compounded with this error in quantifying the overall accuracy of the cross section measurement.

The mean of the set (b) cross sections at 118 eV is 4.5% smaller than that of set (c), but because of the widths of the distributions this was not considered to be significant. Thus any effect of the atom beam energy is neglected and all values at 118 eV were grouped together to obtain an overall mean.

All data from sets (b) and (c) were initially normalised to this mean absolute value at 118 eV and a smooth curve was drawn through the plotted experimental points.

Table 3. Values of cross section for electron impact ionisation of helium obtained from curve fitted to experimental points shown in figure 4.

Mean electron energy (eV)	Cross section (10^{-16} cm^2)	Mean electron energy (eV)	Cross section (10^{-16} cm^2)
26	0.019	58	0.267
26.5	0.024	60	0.275
27	0.031	65	0.293
27.5	0.037	70	0.308
28	0.043	75	0.321
28.5	0.049	80	0.331
29	0.055	85	0.340
29.5	0.061	90	0.348
30	0.066	95	0.354
30.5	0.072	100	0.358
31	0.078	105	0.361
31.5	0.083	110	0.363
32	0.089	115	0.364
32.5	0.094	118	0.365
33	0.099	120	0.365
33.5	0.104	125	0.365
34	0.109	130	0.366
34.5	0.114	135	0.366
35	0.119	140	0.365
35.5	0.125	145	0.363
36	0.129	150	0.362
37	0.139	160	0.358
38	0.148	170	0.354
39	0.156	180	0.349
40	0.164	190	0.344
41	0.172	200	0.339
42	0.179	225	0.325
43	0.187	250	0.312
44	0.194	275	0.300
45	0.200	300	0.288
46	0.207	350	0.266
47	0.213	400	0.245
48	0.220	450	0.227
49	0.225	500	0.213
50	0.230	550	0.200
51	0.236	600	0.189
52	0.240	650	0.179
54	0.250	700	0.170
56	0.259	750	0.162

This is shown as curve I in figure 3. A small discrepancy is apparent between this curve and the data points of set (a) (also plotted in figure 3) and a further adjustment is necessary. Weighted corrections were applied to set (a) (+3.8%) and to the combined sets (b) and (c) (−1.3%) to achieve a best least-squares fit of set (a) to the smooth curve through the points of the adjusted sets (b) and (c). Thus in effect the 27 absolute points of set (a) were utilised to obtain a better absolute value of the cross section at 118 eV to which the data of sets (b) and (c) were renormalised. The renormalised points are shown in figure 4. Because of the effective addition of more data at 118 eV, the 90% confidence limits on the mean value at 118 eV are slightly reduced. At the same time as achieving a better value for the cross section at 118 eV, this procedure allows an optimum curve to be fitted over the whole energy range because the deviations of all sets of data points from a smooth curve are minimised. The curve drawn through the points in figure 4 (also reproduced in figure 3, labelled II) thus represents the best cross section values obtainable from the results of this experiment. The coordinates of the best curve are given in table 3.

The 90% confidence limits of the best curve are a function of energy because the density of data is not constant over the energy range covered. The assessment of the 90% confidence limits is somewhat subjective apart from that at 118 eV where a good statistical analysis is made. The estimated 90% confidence limits given in table 2 include the small contribution from the statistical errors in measuring the ion count rate.

The errors discussed so far are random. They are the result of uncontrolled variations in the surface conditions or small changes in the positions at which the neutral target beam and the He^+ product ions strike their respective detector surfaces combined with the statistical fluctuations in the detected He^+ ion count rate. The overall confidence limits that can be assigned to a value of the ionisation cross section at a particular electron energy arise from a combination of these random errors and the systematic errors due to instrument and detector calibrations and other limitations on the measurements of the parameters in equation (1). These errors have to some extent been discussed already in § 2.2 and are presented in table 1. The total systematic error of ±4.7%, which is essentially independent of electron energy, is obtained by combining the individual systematic errors in quadrature.

4. Discussion

In figure 4 it is seen that the three sets of experimental data, (a), (b) and (c), of the present experiment blend smoothly with each other in the overlapping regions as a result of the iterative normalisation procedure (with respect to absolute data at 118 eV) described in § 3. The smooth curve through the points is monotonic from threshold to 750 eV although the scatter of the points is such that minor structures would not be observed. In the near-threshold region there is no discernible departure from a linear dependence on excess energy above threshold (24.6 eV) for about the first 6 eV when the electron energy distribution (FWHM of 1 eV approximately) is taken into account. The absence of an ionisation signal below threshold is evidence that the beam contains no significant concentration of excited helium atoms.

Figure 4 also shows the data of Rapp and Englander-Golden appropriate for production of He^+, i.e. the small contribution $2Q_2(E)$ of double ionisation (Adamczyk *et al* 1966, Stanton and Monahan 1960) has been subtracted from the total $Q_T(E)$. It can be seen that the general agreement with the present data is very good. It seems likely that the discrepancy previously recorded by Brook *et al* (see figure 3) was caused by over correcting for the effect of ionisation of highly-excited atoms which were

present in their helium beam. Such a correction was not required in the present experiment.

The curve through the present experimental points lies slightly below that of Rapp and Englander-Golden over the whole energy range. The largest difference (about 6%) occurs at about 60 eV and the curves diverge slightly in the high energy region above 500 eV (see the Bethe plot in figure 5). The peak of the cross section lies at

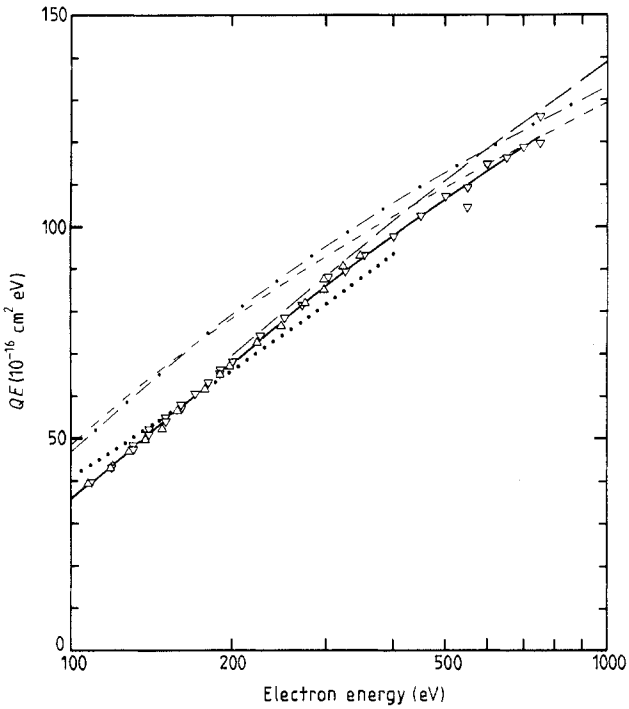

Figure 5. Bethe plot of the cross section for electron impact ionisation of helium. The symbols are identical to those of figure 4. The additional theoretical curves are as follows: —·— Bell and Kingston (1969) (Born approximation); – – – Kim and Inokuti (1971) (Bethe approximation); · · · · Bransden *et al* (1979) (distorted-wave approximation).

about 130 eV where the magnitude of the present data is only 2.2% smaller. The excellent agreement in absolute magnitude is well within the combined errors of the two experiments. This, together with the very close concurrence in the shapes of the two curves, is good evidence that the careful applications of the beam–gas cell technique by Rapp and Englander-Golden and of the fast atom beam technique at Culham are both very reliable. Since the errors of the two sets of measurements are very similiar, we recommend that the cross section for helium should be taken to be the mean of the two curves and the error at a 90% confidence level of this combined curve should be taken to be ±4.5%. Table 4 gives values of this recommended cross section at selected electron energies.

The data obtained by Brook *et al* are plotted in figure 3 and have here been adjusted by +2.4% to correct for a small error in the efficiency of the neutral beam detector†; the method of biassing used in the present study (see appendix) now ensures complete suppression of secondary electron emission in the calibration procedure. The improvement in performance now achieved with the Culham apparatus is clearly demonstrated.

† This correction should also be applied to the data for C, N and O atoms reported by Brook *et al* (1978).

Table 4. Recommended values of cross section for electron impact ionisation of helium (mean of values obtained by Rapp and Englander-Golden (1965) and in present work). The error at a 90% confidence level is estimated to be ±4.5%.

Electron energy (eV)	Cross section (10^{-16} cm^2)	Electron energy (eV)	Cross section (10^{-16} cm^2)
26	0.018	90	0.353
27	0.031	95	0.358
28	0.043	100	0.362
29	0.055	110	0.367
30	0.067	120	0.369
31	0.079	130	0.370
32	0.091	140	0.368
33	0.102	150	0.365
34	0.112	175	0.354
36	0.132	200	0.342
38	0.152	250	0.315
40	0.168	300	0.291
45	0.205	350	0.269
50	0.237	400	0.250
55	0.263	450	0.231
60	0.283	500	0.218
65	0.301	550	0.205
70	0.315	600	0.194
75	0.328	650	0.184
80	0.338	700	0.174
85	0.346	750	0.166

Particularly noticeable is the improvement in the statistical errors, the reduction in the scatter of the experimental points in the near-threshold region, and the absence of a below-threshold ionisation signal. At energies from 40 to 750 eV the data of Brook *et al* are in good agreement with the present data.

Since an outcome of the present study is a strengthening in the confidence of the Rapp and Englander-Golden data, there is little point in commenting upon the many theoretical cross sections† which have previously been compared with that data. An exception to this remark is the high-energy dependence of the present cross section curve, which is particularly clearly shown in the Bethe plot in figure 5. The Born asymptote cross section of Kim and Inokuti (1971) is in good agreement with the present results in the energy range between 500 and 750 eV, although it is apparent that the present data have barely reached the Bethe asymptote at the highest energy of 750 eV; however, the number of data points is small and the scatter is relatively large. It is also worth noting that the high-energy dependence of the present data agrees more closely with theory than does the data of Rapp and Englander-Golden. These observations are also valid for the Bell and Kingston (1969) Born approximation calculation, which is selected for illustration because it is a particularly accurate application of the Born formulation.

At lower energies the distorted-wave calculations of Bransden *et al* (1979) are in good agreement with experiment over the stated range of validity (100 to 400 eV).

† Theoretical work prior to 1968 has been reviewed by Rudge (1968).

5. Conclusion

A new absolute determination of the total cross section for single ionisation of helium atoms by electron impact has been made using the crossed electron–fast atom beam method. The previous problems encountered by Brook *et al* (1978) caused by the presence of highly-excited atoms in the target beam have been eliminated. Over the whole energy range from threshold to 750 eV the measured cross section is in excellent agreement with that measured by Rapp and Englander-Golden (1965) using the traditional beam and gas cell method. We recommend the mean of these two cross sections, with 90% confidence limits of ±4.5%, be adopted as the best data base currently available.

The agreement with the helium ionisation data of Rapp and Englander-Golden provides powerful indirect support for the values of ionisation cross sections of other atoms and molecules measured by Rapp and co-workers (see the review of Kieffer and Dunn 1966).

In the present experiment the overall error achieved in the absolute data is about ±6% and a large part of this error is attributable to drifts in the efficiency of the atom beam detector. There is therefore some potential for improvement in accuracy in fast atom beam experiments by optimisation of this device. The utilisation of an on-line computer has greatly assisted in reducing statistical errors through increasing the amount of data that can be handled, in monitoring the performance of the apparatus, thereby allowing optimisation, and in effectively calibrating the detectors.

Acknowledgments

The authors are grateful for the dedicated and skilled assistance of Mr D Hobbis, Mr P R White, Mr B M White and the late Mr G H Hirst.

Appendix. The atom beam detector

The construction of the atom beam detector is based on the device described by Sharp *et al* (1974). The detector was first used for electron–fast atom beam experiments by Dixon *et al* (1975, 1976). A schematic diagram is presented in figure 6. The aluminium target surface is vacuum-deposited on a 2 μm thick polyester (Mylar) film. On the back surface of the film an antimony and bismuth thermopile with 18 hot and 18 cold

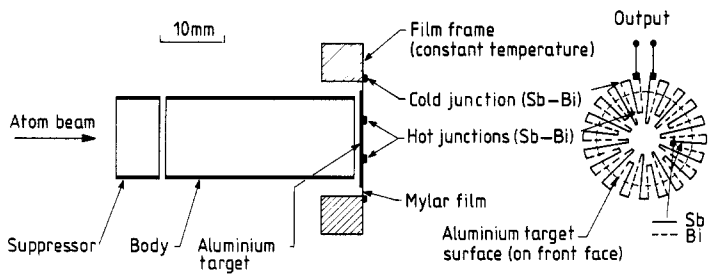

Figure 6. Schematic diagram of the atom beam detector. On the right is shown the pattern of the antimony–bismuth thermopile evaporated on to the back surface of the Mylar film.

junctions is formed by vacuum deposition. The sensitivity is approximately 6 V/W and the time constant is 2 s. The rate of arrival of atoms in a beam of known energy can be determined from the power sensitivity but, because of thermal drift, it was inconvenient during the course of a cross section measurement to make direct use of the thermopile output voltage. Instead, the secondary emission coefficient of the target surface was frequently measured using the thermopile, and during the experiment the current of secondary electrons leaving the surface and collected on the body was used to determine the atom beam intensity. The suppressor cylinder was biassed to −45 V to prevent the loss of secondary electrons and to repel any external slow electrons.

The secondary emission coefficient γ_0 is determined in the following manner.

(1) Ions of known energy E_i are passed into the detector. The body and target surface are connected together and the collected ion current I_i is measured. The voltage ε_i developed by the thermopile is also measured. The power sensitivity $\varepsilon_i / I_i E_i$ can thus be determined.

(2) A beam of atoms of known energy E_0 of the same element as the ion beam in (1) is then passed into the detector. The body is biassed to +45 V to ensure collection of all the secondary electrons emitted by the target. The emission current I_0 and thermopile output ε_0 are measured. The secondary emission coefficient is given by

$$\gamma_0 = \varepsilon_i E_0 I_0 / \varepsilon_0 E_i I_i.$$

During the experiment the detector is connected as in condition (2) and the atom arrival rate I_0 is determined from $I_0 = I / \gamma_0 e$.

References

Adamczyk B, Boerboom A J H, Schram B L and Kistemaker J 1966 *J. Chem. Phys.* **44** 4640–2
Bell K L and Kingston A E 1969 *J. Phys. B: At. Mol. Phys.* **2** 1125–30
Bransden B H, Smith J J and Winters K H 1979 *J. Phys. B: At. Mol. Phys.* **12** 1267–78
Brook E, Harrison M F A and Smith A C H 1978 *J. Phys. B: At. Mol. Phys.* **11** 3115–32
Cook C J and Peterson J R 1962 *Phys. Rev. Lett.* **9** 164–6
Dance D F, Harrison M F A, Rundel R D and Smith A C H 1967 *Proc. Phys. Soc.* **92** 577–87
Dance D F, Harrison M F A and Smith A C H 1966 *Proc. R. Soc.* A **290** 74–93
Dixon A J, von Engel A and Harrison M F A 1975 *Proc. R. Soc.* A **343** 333–49
Dixon A J, Harrison M F A and Smith A C H 1976 *J. Phys. B: At. Mol. Phys.* **9** 2617–31
Eckstein W and Verbeek H 1979 *Max-Planck-Institüt für Plasmaphysik Report* IPP 9–32
Harrison M F A, Smith A C H and Brook E 1979 *J. Phys. B: At. Mol. Phys.* **12** L433–5
Jones T J 1927 *Phys. Rev.* **29** 822
Kieffer L J and Dunn G H 1966 *Rev. Mod. Phys.* **38** 1–35
Kim Y-K and Inokuti M 1971 *Phys. Rev.* A **3** 665–78
Rapp D and Englander-Golden P 1965 *J. Chem. Phys.* **43** 1464–79
Rudge M R H 1968 *Rev. Mod. Phys.* **40** 564–90
Sharp L E, Holmes L S, Stott P E and Aldcroft D A 1974 *Rev. Sci. Instrum.* **45** 378–81
Stanton H E and Monahan J E 1960 *Phys. Rev.* **119** 711–5
Tate J T and Smith P T 1932 *Phys. Rev.* **39** 270